NJC

PAPER

View Article Online
View Journal

Cite this: DOI: 10.1039/c4nj01755b

Cystine-derived bis-naphthalimides as stimuli-responsive fluorescent gelators†

Rupam J. Sarma* and Kakali Devi

Received (in Porto Alegre, Brazil) 8th October 2014,
Accepted 17th March 2015

DOI: 10.1039/c4nj01755b

www.rsc.org/njc

Two cystine-derived bis-naphthalimide gelators (**L1**, **L2**) were synthesised and characterised. Both **L1** and **L2** exhibited similar absorptions and emission spectra in solvents such as acetonitrile and DMF. The fluorescence spectra of both the compounds featured a distinct monomer and long-wavelength excimer emissions in the aforementioned solvents. It was found that the excimer emissions for the two compounds could be preferentially quenched by triethylamine, and subsequently restored with hydrofluoric acid. The stimuli-responsive nature of the excimer emissions was demonstrated using anion stimuli in solution and in the gel phase. Thus, the excimer emission for **L1** (or **L2**) could be switched 'off' using fluoride anions, and subsequently re-activated using tetrafluoroborate anions as the chemical stimulus.

1. Introduction

The versatile luminescent characteristics of naphthalimide derivatives have evoked immense interest, which is evidenced by the frequent use of this fluorophore in optoelectronic materials,[1–4] as ionophoric sensors/probes[5–9] and in stimuli-responsive systems.[10,11] Typically, a stimuli-responsive system should be able to recognize an external stimulus (*e.g.* physical or chemical input), evaluate the inputs, and then respond through changes in its physical and/or chemical characteristics.[2,10,11]

Among the various stimuli-responsive systems identified to date, the importance of low molecular-weight gelators has grown significantly owing to their potential applications as functional materials.[12,13] In addition to being thermo-sensitive, these materials exhibit dynamic self-assembling characteristics, which could be triggered by solvents,[14] light,[15] sound,[16] pH[17] and ionic species.[18] An important challenge in this regard has been the development of stimuli-responsive gelators, which are capable of reversibly interacting with cations and anions, with concomitant fluorescence switching.[13,19]

The presence of two naphthalimide motifs in close proximity (*i.e.* bis-naphthalimides) can generate monomer and excimer emissions, depending on the solvent, molecular environment and distance separating the fluorophores.[20,21] In addition to these factors, the monomer/excimer emissions of bis-naphthalimide derivatives can also be modulated by the coordination of metal ions and self-aggregation.[11,19] For instance, bis-naphthalimide ligands that exhibit an unusual enhancement in the intramolecular excimer fluorescence upon metal ion coordination[10,12] could be developed as potential sensors for Cu^{2+}, Hg^{2+} and Zn^{2+}.

Because naphthalimide emissions are also environment-sensitive, this fluorophore has been utilised as luminescent turn-on probes for studying ligand–cation interactions[22,23] and in bio-sensing.[24–26] However, compared to metal ions, the interactions of bis-naphthalimides with halide anions, particularly fluoride, and the effect of such interactions on their monomer/excimer emissions remain relatively elusive.[27–29]

An important question in this regard is the examination of how the bis-naphthalimide motif would respond to anionic stimuli (*e.g.* fluoride anions), in solution and in the gel phase, and whether these interactions could result in perceptible changes in their fluorescent profiles. For this purpose, we synthesized and characterised two L-cystine-based bis-naphthalimides, **L1** and **L2** (Scheme 1) and then evaluated their fluorescent responses with regard to acid–base and anion stimuli.

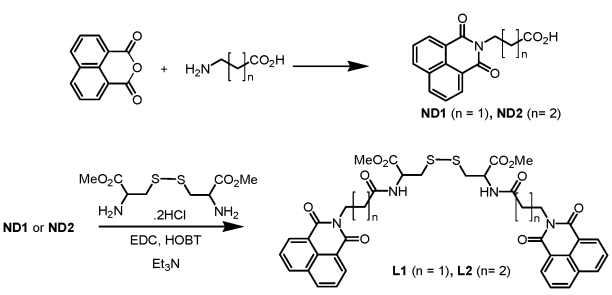

Scheme 1 Synthesis of bis-naphthalimides **L1** and **L2**.

Department of Chemistry, Gauhati University, Guwahati, 781014, Assam, India. E-mail: rjs@gauhati.ac.in; Fax: +91 36125 70535; Tel: +91 98641 28514

† Electronic supplementary information (ESI) available: Details of synthesis, characterisation; SEM images for **L1**; ^{1}H NMR studies of **L1** with $NaBF_4$; fluorescence titration plots of **L1** and chloride, bromide and acetate. See DOI: 10.1039/c4nj01755b

2. Experimental

2.1 Materials and methods

All the chemicals were commercially available from Sigma-Aldrich or Spectrochem (India) and were used as received. Solvents for spectroscopic experiments were distilled under nitrogen atmosphere before use. All the ^{1}H and ^{13}C NMR spectra were obtained on a 300 MHz Bruker spectrometer, and reported in δ per ppm. The electronic absorption spectra were recorded on a Shimadzu UV-vis spectrophotometer (Model UV-1800), and fluorescence spectra were recorded using a Hitachi F2500 fluorimeter.

2.2 Synthetic procedures

Synthesis of ND1 and bis-naphthalimide L1. ND1: naphthalene-1,8-dicarboanhydride (2.011 g, 10 mmol) was mixed with β-alanine (1.063 g, 10 mmol) in a round bottom flask equipped with a magnetic needle. To this mixture, DMF (10 mL) was added and the resulting mixture was allowed to stir at 80 °C for about 12 h. Initially, the colour of the mixture was brown, and after 12 h, a homogeneous red solution was obtained. Subsequently, the reaction mixture was concentrated and cooled to 0 °C, which produced **ND1** as pale yellow crystals (yield 69%). ^{1}H NMR (300 MHz, DMSO-d$_6$/CDCl$_3$) δ_H 8.48 (d, 2H, J = 6.9 Hz), 8.16 (d, 2H, J = 6.9 Hz), 7.67 (t, 2H, J = 7.5 Hz), 4.36 (t, 2H, J = 7.2 Hz), 2.6 (t, 2H); ^{13}C NMR (75 MHz, DMSO-d$_6$/CDCl$_3$) δ 173.20, 163.81, 133.89, 131.42, 131.07, 127.98, 126.75, 122.35, 35.98, 32.32.

Bis-naphthalimide, **L1**: to a solution of **ND1** (0.540 g, 2.0 mmol) in dichloromethane (10 mL), *N*-(3-dimethylaminopropyl)-ethylcarbodiimide hydrochloride (EDC·HCl) (0.400 g, 2.1 mmol) and 1-hydroxybenzotriazole (HOBT) (0.27 g, 2 mmol) were added and the mixture was allowed to stir at 0 °C for 30 min. To this mixture, L-cystine methyl ester dihydrochloride (0.341 g, 1.0 mmol) and triethylamine (0.7 mL, 5.0 mmol) were added and the mixture was allowed to stir for 12 h. After the reaction was complete, the mixture was concentrated under vacuum, and a viscous material was obtained. The addition of water afforded a pale yellow solid, which was filtered, and rinsed with distilled water. The solid product was recrystallised from acetone, and dried in air. Yield 84%, ^{1}H NMR (300 MHz, DMSO-d$_6$) δ 8.59 (2d, amide NH), 8.39 (4H, m), 7.82 (1H, t, J = 7.2 Hz), 4.55 (1H, bm), 4.22 (2H, s), 3.61 (3H, s), 3.336 (H_2O), 3.050 (3H, s), 2.960 (3H, s), 2.933 (2H, m), 2.489 (2H, s). ^{13}C NMR (75 MHz, DMSO-d$_6$): 171.79, 171.06, 164.17, 135.12, 132.12, 131.52, 128.22, 128.03, 122.96, 53.07, 52.14, 37.21, 34.14; FT-IR (cm^{-1}): 3448 (amide NH), 3304, 1743 (ester C═O), 1701, 1649 (amide C═O), 1587; ES-MS: m/z 793.81, calc. for (M + Na$^+$)

Synthesis of ND2 and bis-naphthalimide L2. ND2: naphthalene-1,8-dicarboanhydride (2.981 g, 15 mmol) was mixed with 4-aminobutyric acid (1.556 g, 15 mmol) in a round bottom flask equipped with a magnetic needle. To this mixture, DMF (30 mL) was added and the resulting mixture was allowed to stir at 80 °C for about 12 h. The colour of the mixture at the time of mixing was brown. After about 12 h, a homogeneous yellow-brown solution was obtained. The desired product, **ND2**, was crystallised after the solution was placed in an ice bath. The solid compound was filtered, and washed with EtOH–water to afford a yellow solid. Yield 74%; ^{1}H NMR (300 MHz, DMSO-d$_6$/CDCl$_3$) δ 8.3 (d, 2H), 8.0 (d, 2H), 7.5–7.4 (t, 2H), 4.0–3.9 (t, 2H);^{13}C NMR (75 MHz, DMSO-d$_6$/CDCl$_3$) 174.53, 163.74, 133.75, 131.20, 130.80, 127.69, 126.62, 122.12, 40.51, 40.23, 39.95, 39.67, 39.39, 39.22, 39.11, 38.83, 31.44, 23.15.

Bis-naphthalimide, **L2**: as described for **L1**. The recrystallised product was obtained as a pale yellow solid. Yield 75%. ^{1}H NMR (300 MHz, CDCl$_3$) δ_H 8.54 (4H, d, J = 7.2 Hz), 8.15 (4H, d, J = 7.5 Hz), 7.71 (4H, t, J = 7.5 Hz), 7.06 (2H, amide NH), 4.90 (2H, m, J = 4.2 Hz), 4.25 (2H, m, J = 4.5 Hz), 3.75 (3H, s), 3.24 (4H, d, J = 5.1 Hz), 2.39 (4H, t, J = 4.8 Hz), 2.14 (4H, m), 1.65 (residual H_2O). ^{13}C NMR (75 MHz, CDCl$_3$): 172.33, 171.0, 164.31, 133.97, 131.43, 131.31, 128.0, 126.89, 122.36, 77.41, 52.69, 51.72, 40.57, 39.50, 33.66, 24.14. FT-IR (cm^{-1}): 3310 (amide NH), 1740 (ester C═O), 1693 (amide C═O), 1657, 1587; ES-MS: m/z 821.85, calc. for (M + Na$^+$)

Gel formation with L1 and L2. In a typical gelation experiment, a known amount of the bis-naphthalimide gelator (3 mg mL^{-1} for **L1** and 5 mg mL^{-1} for **L2**) and solvent (1.00 mL) were mixed in a screw-capped glass vial and maintained at 80 °C for 2 h. In the process a clear solution was obtained, which upon cooling to room temperature over a period of time (~2 h) led to gel formation. Moreover, the gelation of **L2** in chloroform, acetonitrile, DMF and DMSO could be triggered by ultra-sonic irradiation for 2–3 minutes. The stability of the organogel was tested using the "inversion" method.

3. Results and discussion

3.1 Synthesis and characterisation of L1 and L2

In a typical experiment, **ND1**, was synthesised by condensing naphthalene-1,8-dicarboanhydride (1,8-NDA) and 3-aminopropanoic acid, and then it was coupled to L-cystine methyl ester using EDC–HOBT coupling strategies (Scheme 1); the desired bis-naphthalimide **L1** (or **L2**) was obtained as a solid, and characterised using ^{1}H/^{13}C NMR and mass spectroscopy.

The UV-visible absorption spectra of **L1** (Fig. 1a) and **L2** were markedly similar, both exhibited absorptions at 334 nm with a shoulder at 346 nm. In addition, the fluorescence spectra of the two compounds also displayed similar features. For instance, when irradiated at 340 nm in acetonitrile, bis-naphthalimide, **L1**, produced two emissions at 381 nm and 465 nm (Fig. 1b); of these,

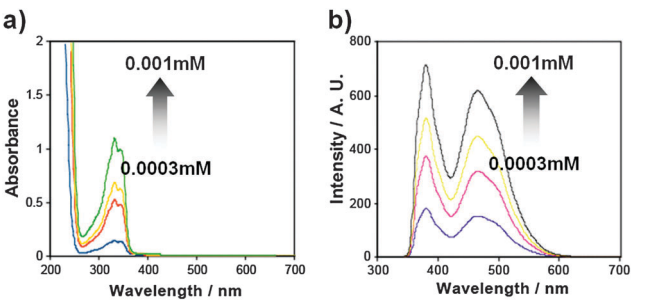

Fig. 1 Concentration-dependent (a) UV-visible and (b) fluorescence spectra of **L1** in MeCN.

the emission at 381 nm is characteristic of the naphthalimide monomer, while the broad emission at 465 nm is attributed to the intramolecular dimerisation of the naphthalimide motifs.[20,30,31] The formation of intramolecular naphthalimide dimers (*i.e.* excimers) could be recognised from the relative intensities of the monomer–dimer emissions at 381 nm and 465 nm, the ratio of which was almost constant ($I_{381/465}$ = 1.16 ± 0.15) for concentrations up to 0.015 mM.[30,31] Similarly, the irradiation of **L2** at 340 nm in acetonitrile produced two emissions at 382 nm and 467 nm, which correspond to the naphthalimide monomer and excimer emissions. Notably, the observation of intramolecular excimers for **L1** and **L2** was in accordance with the previous reports of bis-(1,8-naphthalimide) with flexible oligomethylene spacer groups.[20,32,33] The formation of intramolecular naphthalimide dimers (*i.e.* **L1** and **L2**) in the ground state was in agreement with the fact that the excitation spectra obtained in both the cases were similar.[30]

With this perspective, we inferred that the excimer emissions for **L1** and **L2** originate from the intramolecular dimerisation of the naphthalimide motifs in the ground state. As will be discussed later, the formation of such excimers was possibly favoured by intramolecular hydrogen bonds invoked by the amide NH groups, and the hydrophobic interactions between the naphthalimide groups, given the conformational flexibility of the cystine disulfide group. Moreover, it can be pointed out that the formation of intramolecular excimers between the two naphthalimide motifs for **L1** and **L2** (>12 C–C bonds) was comparable to the previous reports for bis-naphthalimides linked by oligoethylene spacers.[21,27]

The effects of spacer groups on excimer fluorescence have been illustrated earlier by the development of bis-naphthalimide ligands for cation binding. In a related example, intramolecular excimer emissions (at 470 nm) were reported for the complexes of $Zn(OTf)_2$ with naphthalimide–imine ligands, in which excimer switching could be observed, depending on the metal/ligand stoichiometry.[34] Again, intramolecular excimer formation was observed after the dimerisation of *N*-benzocrown derived naphthalimides, which was apparently induced by the coordination of Ba^{2+} cations.[11] Given these spectral features, we were curious to examine the prospect of anion-induced switching of excimer emissions in relation to the monomer emissions of the bis-naphthalimides.

3.2 Effects of acid–base stimuli on L1 and L2

In a related study, we noted that the addition of a 3°-amine (*i.e.* triethylamine) to bis-naphthalimides **L1** (or **L2**) triggered a reduction in their emission profiles, particularly the long-wavelength excimer emission. As shown in Fig. 2, the addition of triethylamine to **L1** led to the substantial quenching of the 465 nm emission, compared to the monomer emission at 381 nm. This result is understandable because the amino-groups have been known to induce the quenching of long-wavelength emissions *via* photo-induced electron transfer (PET), as reported earlier for naphthalimide(-spermine) derivatives.[30,35]

Following this, we examined the influence of acid on the **L1**–triethylamine mixture, anticipating that the protonation of the 3°-amine would block the incipient PET process, and hence

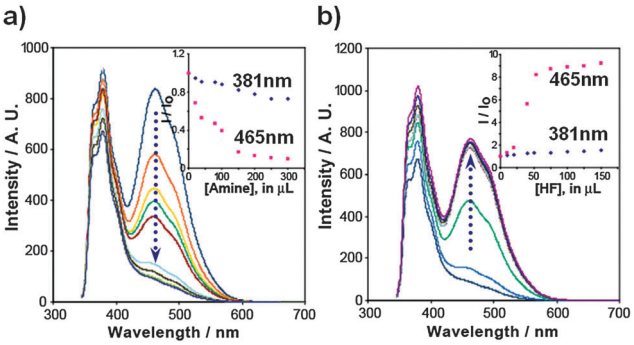

Fig. 2 (a) Effect of triethylamine (1.5 mM) on the fluorescence emission of **L1** (0.001 mM, MeCN), followed by (b) hydrofluoric acid (aq., 3.0 mM) on the **L1**–triethylamine mixture; (inset: plots of I/I_0 *vs.* [triethylamine] and [HF], for the emissions occurring at 381 nm and 465 nm).

restore the excimer fluorescence at 465 nm. Accordingly, the **L1**–triethylamine solution was titrated using hydrofluoric acid (aq. HF, 3.0 mM); the emission spectra obtained during the acid titration clearly revealed that the acid stimulus could switch 'on' the excimer emissions at 465 nm (Fig. 2b). Moreover, using the same amine–acid combination as stimuli, we could induce multiple cycles of reversible quenching and restoration of the 467 nm emissions of **L2** in acetonitrile.

The amine-induced quenching of the excimer emissions of **L1** and **L2** could also be observed in solvents such as DMF and DMF–water. This result is in accordance with the suggestion that the fluorescence behaviour of substituted naphthalimides can be influenced by protons, and/or by changes in pH.[10,31] These features were complementary to two-step fluorogenic switches, demonstrated for 2°-amine derived, intramolecularly quenched bis-naphthalimide systems, which could be activated using protons as inputs.[36,37]

3.3 Effects of anions on the fluorescence responses of L1 and L2

Notwithstanding the acid/base or proton-dependent switching of naphthalimide fluorescence in **L1** and **L2**,[38,39] we were curious to examine the effects of fluoride (*i.e.* TBAF) as anion stimuli on the monomer/excimer fluorescence of the bis-naphthalimide derivatives, and hence compare the influence of halide anions, including BF_4^- anions.

Accordingly, we performed the fluorescence titrations of bis-naphthalimide **L1** with fluoride anions (*i.e.* TBAF) in acetonitrile. As shown in Fig. 3a, the incremental addition of fluoride (up to 20 equiv.) to **L1** caused the emission intensity at 465 nm to gradually diminish, whereas the monomer emission at 381 nm increased 2-fold.[40] Notably, the changes in fluorescence at 381 nm and 465 nm for **L1** with increasing fluoride concentration were such that $I_{381/465}$ increased to 18.3. Although the effects of other halide anions on the excimer fluorescence were minor, we noted distinct fluorescence enhancements for BF_4^- anions. Surprisingly, the addition of BF_4^- anion (~50 equiv.) to **L1**/TBAF produced an enhancement in both the monomer and excimer emissions (as seen in Fig. 3b). This enhancement of excimer fluorescence is unusual because it appeared to override the quenching effects of the fluoride anions, due to which the

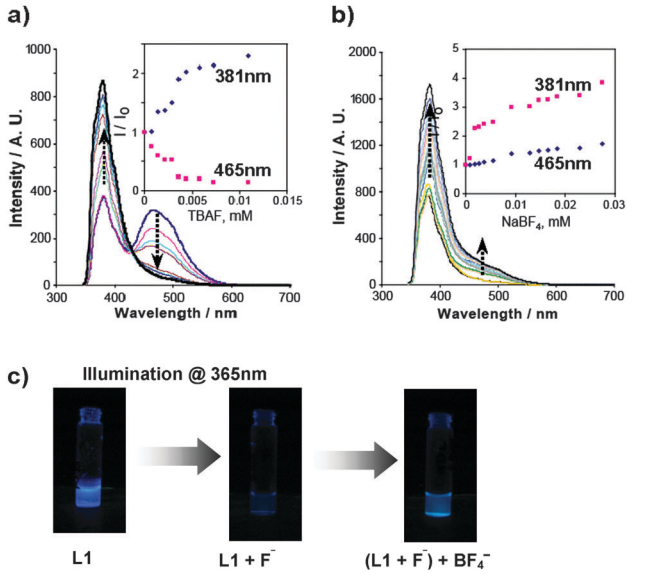

Fig. 3 Variations in the fluorescence emissions at 381 nm and 465 nm for **L1** (0.0005 mM; acetonitrile) (a) upon the addition of TBAF (inset shows rel. changes in emissions, I/I_0 *vs.* [TBAF], at 381 nm and 465 nm); (b) following the addition of BF_4^- anions to the **L1**–TBAF mixture (inset shows the rel. changes in fluorescence, I/I_0 *vs.* [$NaBF_4$], at 381 nm and 465 nm); (c) changes in the emissions of **L1** upon successive addition of TBAF, and $NaBF_4$, as viewed under UV-illumination (365 nm).

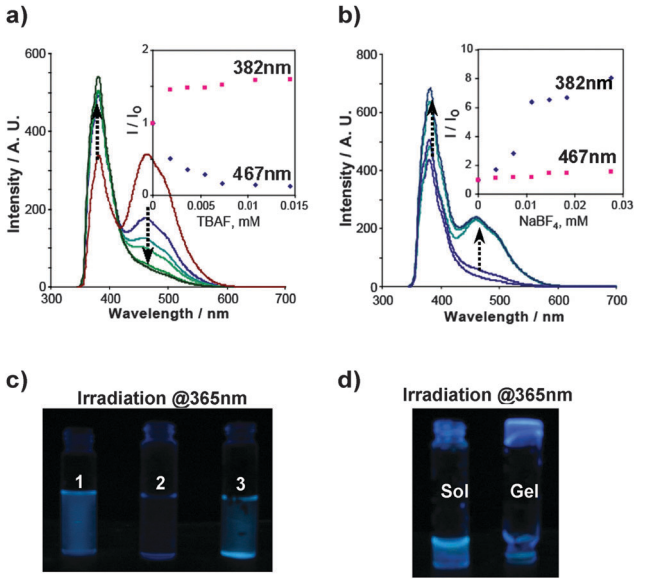

Fig. 4 (a) Gradual disappearance of the excimer emission of **L2** (0.0004 mM; acetonitrile) at 467 nm upon addition of TBAF; (b) excimer emission at 467 nm 'restored' following the addition of BF_4^- anions to the **L2**–TBAF solution; (inset: rel. changes in emissions, I/I_0 *vs.* [TBAF], and then [$NaBF_4$] monitored at 382 nm and 467 nm); (c) fluorescence profiles of **L2** ('**1**') following successive addition of TBAF ('**2**') and $NaBF_4$ ('**3**') in acetonitrile, as observed under UV-illumination (365 nm). (d) Fluorescence emission of **L2** in acetonitrile solution and in the gel-state (5 mg mL^{-1}, acetonitrile), when illuminated with 365 nm light.

465 nm emission was 'switched-off'. Furthermore, the changes in the fluorescence output of **L1** brought about by the addition of fluoride anions, and subsequent addition of BF_4^- anion could be monitored visually under 365 nm illumination (Fig. 3c).

Similarly, we monitored the fluorescence responses of **L2**, in acetonitrile, subsequent to the addition of fluoride anions. As shown in Fig. 4, the incremental addition of the fluoride anion to **L2** was accompanied by a gradual disappearance of the excimer emission (467 nm), while the monomer emission at 382 nm increased 1.5 times, with saturation at 25 equiv. of the anion. Furthermore, the addition of BF_4^- anions ($\sim$55 equiv.) to the solution of **L2**–TBAF caused the excimer emission at 467 nm to be restored, analogous to **L1**.

The abovementioned results, *viz.*, quenching of the excimer emissions of **L1** and **L2** in the presence of fluoride anions, could be analysed as follows: first, the interaction of fluoride anions with the amide NH groups (of **L1** and **L2**) could disrupt the formation of intramolecular excimers between the naphthalimide motifs.[40] Indeed, the quenching of the excimer fluorescence in naphthalimides through fluoride-induced disruption of intramolecular hydrogen bonds has been reported earlier.[41] Alternatively, the anion–π interactions of the proximal fluoride with the naphthalimide motif could facilitate a partial PET process, thereby leading to the quenching of the excimer fluorescence.[30,36]

Second, the quenching effects of fluoride anions were rather supressed in polar solvents such as aqueous DMF and in the presence of MeOH. This indicates that in protic solvents, such as MeOH or aqueous DMF, the electronegative fluoride anions would preferably be hydrated, than the hydrogen bond to the amide NH group of the bis-naphthalimide. In this context, the effects of chloride, bromide and acetate anions on the bis-naphthalimide fluorescence were relatively minor, although acetate anions produced minor quenching of excimer emissions (Fig. S14 and S15; ESI†) under identical conditions.[42]

Moreover, the enhancement of monomer emissions in both the cases, **L1** and **L2**, following the addition of fluoride and BF_4^- anions was notable. Again, compared to the highly electronegative fluoride anion, the effects of BF_4^- anions were expected to be relatively soft and unlikely to form strong hydrogen bonds. Although the precise nature of the interactions of BF_4^- with the bis-naphthalimide was not clear, we inferred that the BF_4^- anion could assist the dimerisation of the naphthalimide motifs[43] and impede the fluoride-induced PET process. This proposition seems reasonable given the results obtained from the FTIR and ^{1}H NMR investigations of the **L2**–$NaBF_4$ system. The effect of the fluoride anion on the emissions of **L1** (or **L2**) was also illustrated using NaF; despite its low solubility, the addition of NaF to bis-naphthalimide induced quenching of the excimer emission, albeit minor compared to TBAF. This quenching of the excimer *vis-à-vis* monomer emissions by NaF could subsequently be reversed upon the addition of BF_4^- anions.[44]

3.4 Stimuli-responsive fluorescent gels from L1 and L2

Interestingly, both the bis-naphthalimides, **L1** and **L2**, produced fluorescent gel phases in DMSO and DMF;[45] in the case of DMSO, the critical gelation concentrations (CGC) were found to be 3 mg mL^{-1} for **L1** and 5 mg mL^{-1} for **L2**. Fig. 5a and b show the scanning electron microscopic (SEM) images of the

gels obtained from **L1** and **L2** in DMSO, which indicated the formation of fibrous networks involving the gelator molecules.

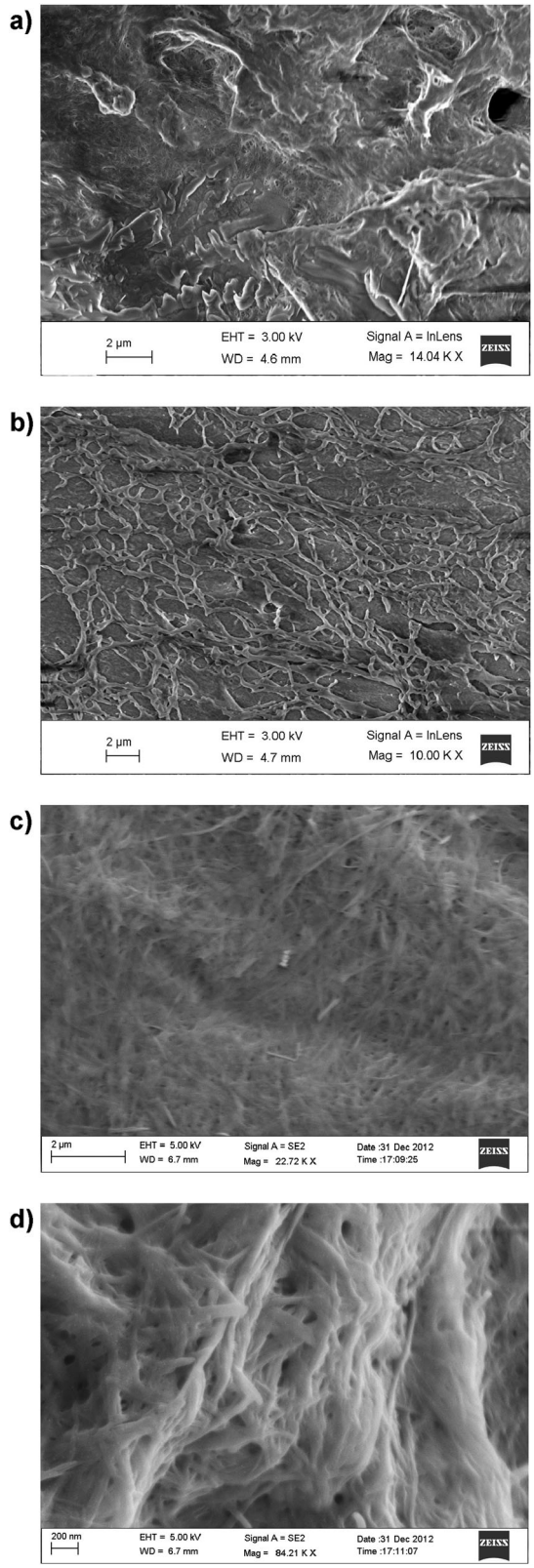

Fig. 5 SEM images of the dried organogel obtained from: (a) **L1** in DMSO; (b) **L2** in DMSO; (c), (d) **L2**/DMF gel under different magnifications.

Similar self-assembled entangled networks could be visualised in the case of the **L2**/DMF gel (Fig. 5c and d), and the **L2**/acetonitrile gel, which, on close inspection, revealed fibres with dimensions >2 μm. The critical gelation concentrations for **L1** and **L2** in DMF were found to be 3 g mL^{-1} and 6 mg mL^{-1}, respectively. Moreover, **L2** produced thermo-reversible gels in chloroform and acetonitrile, which could also be triggered by ultra-sonic treatment.[45]

Preliminary insights into the nature of the intermolecular interactions in the gel phase *vis-à-vis* solution could be obtained from fluorescence experiments. For instance, the **L2**/DMF organogel was characterised by emissions at 399 nm and 468 nm, respectively, whereas the corresponding emissions for **L2** (0.004 mM) in dilute DMF solution occurred at 382 nm and 460 nm (Fig. S11, ESI†). Such red-shifting of the fluorescence emissions were evident for both **L1** and **L2** in the gel phases, as compared to the solution. In particular, the red-shifts observed in the emission spectra for **L2** in the gel state are consistent with the weak aromatic–π interactions of the naphthalimide motifs.[13,42] **L1** and **L2** exhibit red-shifted excimer emissions, particularly in the gel state,[46] which also provided support to the possible intramolecular dimerisation of the pendent naphthalimide groups.[47,48]

We propose that the gelation process involving bis-naphthalimide, **L2**, (or **L1**) could be driven by multiple supramolecular interactions, *viz.*, intermolecular hydrogen bonding involving the amide and naphthalimide groups and π–π interactions between the naphthalimide motifs. While the red-shifting of fluorescence emissions in the gel state suggested aromatic–π stacking between the naphthalimide motifs, we reasoned that FTIR and ^{1}H NMR studies could provide valuable insights into the driving forces for gel formation.

In order to examine the effect of hydrogen bonding interactions on the gelation process, we performed the FTIR analysis of **L2** in chloroform/acetonitrile. In dilute solution, the FTIR spectra of **L2** (0.1 mg mL^{-1}) indicated a distinct amide NH absorption at 3303 cm^{-1}; the absorption at 3303 cm^{-1} remained relatively unaffected within the gelator [**L2**] = 1.0 mg mL^{-1}, and emanated from intramolecular hydrogen bonds involving the amide NH groups. However, at [**L2**] = 2.0 mg mL^{-1}, a broad absorption appeared at 3470 cm^{-1} in chloroform/acetonitrile, which shifted further to 3440 cm^{-1} with substantially broadening upon gel formation (Fig. S16, ESI†), indicating the formation of extensive hydrogen bonded networks.

The crucial role of hydrogen bonding during the gelation process was also investigated using ^{1}H NMR in chloroform-d and acetonitrile-d_3. In this regard, the interactions of fluoride with bis-naphthalimide as described in previous sections could also be substantiated, particularly for **L2** in chloroform-d and acetonitrile-d_3.

As indicated by ^{1}H NMR, increasing the concentrations of **L2** from 0.3 mg mL^{-1} to 2 mg mL^{-1} in chloroform-d did not significantly affect either the naphthalimide CH or amide NH resonances (Fig. S19, ESI†). Given that the hydrogen bonding tendency of chloroform under these conditions is limited, we anticipated that the intra-molecular hydrogen bonds between

the amide NH groups would persist. These features were consistent with the observations made in the FTIR spectra for **L2** in chloroform. At a higher concentration of **L2** (CGC = 5 mg mL^{-1}, with ultra-sonic irradiation) gel formation was observed, and the naphthalimide CH resonances at 7.72, 8.17, and 8.57 ppm shifted slightly upfield ($\Delta\delta \sim 0.01$ ppm), which was reminiscent of the weak intra-molecular interactions between the naphthalimide motifs. Though the amide NH resonance appeared to be invariant up to 1.0 mg mL^{-1}, gelation caused this resonance to shift slightly downfield from 7.07 ppm to 7.09 ppm, possibly indicating an extended hydrogen bonding situation. Thus, a clear correlation can be seen in the behaviour of the amide NH groups, with regard to intra-molecular hydrogen bonding, both from the FTIR and ^{1}H NMR studies. Therefore, we inferred that the formation of the **L2**/chloroform gel was driven by aromatic π-stacking interactions, assisted by hydrogen bonding interactions between the amide NH groups. Further support to the hydrogen bonding condition of amide NH groups could be obtained by the gradual addition of TBAF (up to 3 equiv.) to the **L2**/chloroform gel, which caused a downfield shift of the amide NH resonance from 7.09 to 7.23 ppm (Fig. S20, ESI†) with partial dissolution of the gel.

Following this, we sought to examine the effect of gelation on the naphthalimide CH and amide NH groups of the **L2**/acetonitrile gel using ^{1}H NMR spectroscopy. Because **L2** caused the rapid gelation of acetonitrile, it seemed pertinent to carry out temperature-dependent ^{1}H NMR analysis of the **L2**–acetonitrile-d_3 system.

As shown in Fig. 6, the solution of **L2** in acetonitrile-d_3 at 50 °C produced a distinct set of resonances for the naphthalimide CH protons at 7.70, 8.20 and 8.42 ppm along with a minor set of resonances at 7.82, 8.34 and 8.54 ppm, respectively; the integrated ratios for the major and minor signals were found to be ~9 : 1. At 50 °C, the minor resonances were attributed to the **L2** molecules in the incipient gel,[47] while the major resonances at 7.70, 8.20 and 8.42 ppm, emanated from the solvated **L2** molecules. In other words, the two sets of resonances produced by the naphthalimide CH groups in acetonitrile (*cf.* in chloroform the signals were minor), were reminiscent of the inequivalence of the naphthalimide motifs in the solution/sol state *vis-à-vis* the gel phase.[47]

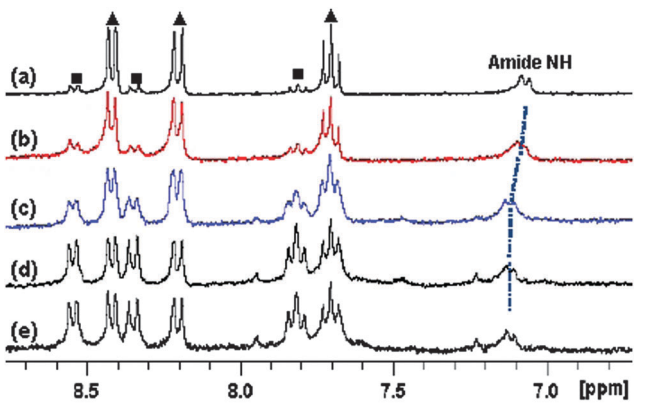

Fig. 6 Partial ^{1}H NMR spectra of **L2** (5 mg mL^{-1}) showing the temperature-dependent variations of the naphthalimide CH and amide NH resonances in acetonitrile-d_3: (a) 50 °C; (b) 45 °C; (c) 35 °C; (d) 25 °C; (e) 25 °C after 12 h; (the two sets of naphthalimide CH resonances could be attributed to the inequivalence of the naphthalimide motifs in the solution/sol state, designated as '▲' *vis-à-vis* the gel phase, indicated as '■'). The increase in temperature could lead to disruption of hydrogen bonds involving the amide NH groups, which accounted for the gradual upfield shifting of the resonances.

With a decrease in the temperature, the set of naphthalimide CH resonances at 7.82, 8.34 and 8.54 ppm gradually gained prominence. Thus, the intensities of the two sets resonances became almost comparable at 25 °C, and concomitantly gelation was initiated. The gradual changes observed in the naphthalimide CH resonances as a function of temperature (Fig. 6), reflects the importance of the aromatic–π interactions during the gelation process. It was noted that gel formation was accompanied by the appearance of an additional signal due to the aliphatic CH groups connected to the naphthalimide motif (Fig. S21, ESI†). However, the effect of gelation on the amide NH resonances of **L2** was minor, with a gradual shift from 7.07 ppm in solution (50 °C) to 7.12 ppm in the gel phase. With an increase in temperature, the amide NH resonance (of **L2**) was shifted upfield; such changes could be explained by the breaking of the intermolecular hydrogen bonds associated with the amide NH group, *viz.* with the solvent and neighbouring gelator molecules.

As illustrated in Scheme 2, the emergence of downfield shifted resonances for the naphthalimide CH protons at 7.82, 8.34 and 8.54 ppm following gel formation was illuminating because it corroborated the presence of **L2** both as solvated species and in the gel phase. Moreover, noteworthy was the splitting/broadening of these resonances due to the cys-methyl ester group, which could be correlated to the proximal interactions of this residue with the naphthalimide motifs groups during the formation of the **L2**/acetonitrile organogel (Fig. S21, ESI†). The temperature-dependent self-assembling process of **L2** in acetonitrile clearly reflected the importance of the aromatic–π stacking interactions in its gelation behaviour, which was supplemented by hydrogen bonds between the gelator molecules. Based on the results of the ^{1}H NMR experiments, and given the red-shifted emissions observed for **L2** in the gel phase, it seems reasonable that the naphthalimide motifs interact in a head-to-tail manner in the gel phase.[13,46]

Moreover, as monitored by ^{1}H NMR, the onset of gelation for **L2**/acetonitrile-d_3 (or chloroform-d) was marked by lower intensity signals, compared to those in solution. This is understandable because the formation of the **L2**/acetonitrile gel restricted a larger proportion of **L2** gelator molecules to enter the gel structure, thereby reducing the thermal motions of the gelator molecules.[48]

On the basis of these observations, it is inferred that the self-assembly of the gelator molecules of **L2**, in acetonitrile or chloroform is driven by aromatic–π stacking between the naphthalimide motifs and supplemented by hydrogen bonds involving the amide NH groups (Scheme 2). As mentioned earlier, the FTIR analysis indicated the presence of intramolecular hydrogen bonds in **L2**, which in turn could explain the observations of excimer emission in the fluorescence spectra. This intramolecular nature of the incipient hydrogen bonds was also reflected in the ^{1}H NMR spectra, with the amide NH resonances

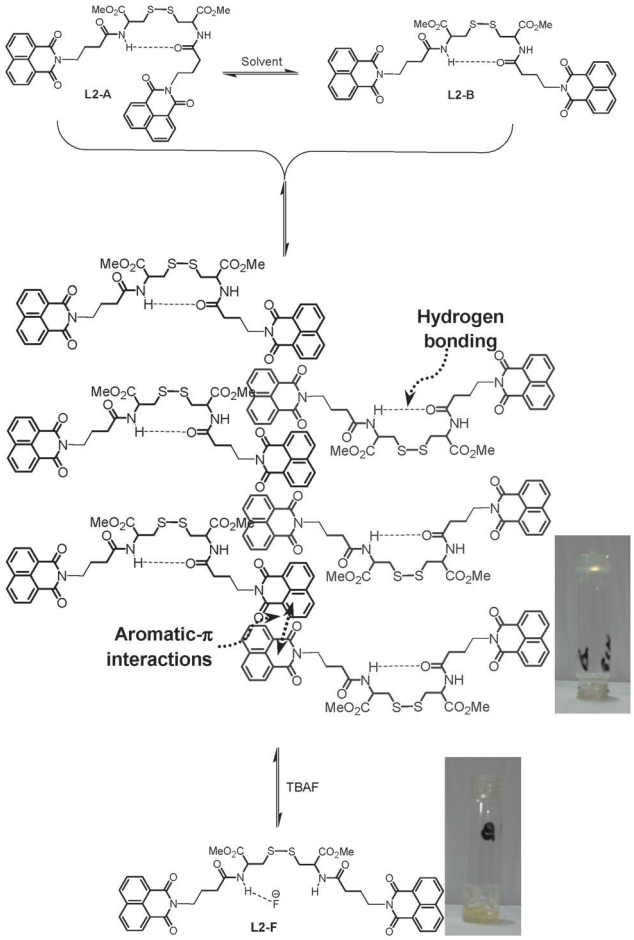

Scheme 2 Formation of intramolecular hydrogen bonds for **L2** in solvents such as acetonitrile, showing the plausible interaction of the F^- anions (*i.e.* TBAF) with the bis-naphthalimide; The importance of aromatic–π and hydrogen bonding interactions between the gelator molecules during gel formation and fluoride-induced gel-to-sol transformation have been illustrated (inset: photographic images of the **L2**/acetonitrile gel and solution [**L2**] = 5 mg mL^{-1}).

showing only minor downfield shifts. Considering these aspects, we inferred that hydrogen bonding between the amide NH groups were favored when the gelator molecules adopted bent conformations. Previous studies have shown the importance of intramolecular hydrogen bonding interactions during the formation of self-assembled gels, and how such interactions were favored when the gelator molecules adopted bent conformations.[47] Again, these polar interactions facilitated the hydrophobic packing of the naphthalimide groups (Scheme 2), such that the gelator molecules slowly self-assembled into entangled fibrous networks.[47] In fact, the influence of the hydrophobic aromatic–π interactions between the naphthalimide groups and segregation of hydrophilic interactions during the gel formation process was recently reported.[46,48]

Similar gel-to-sol transformations were noted for the **L2**/acetonitrile gels, upon the addition of TBAF, which was also accompanied by the quenching of the excimer fluorescence. We reasoned that the gel-to-sol transformations emanated from the disruption of the hydrogen bonded network involving the

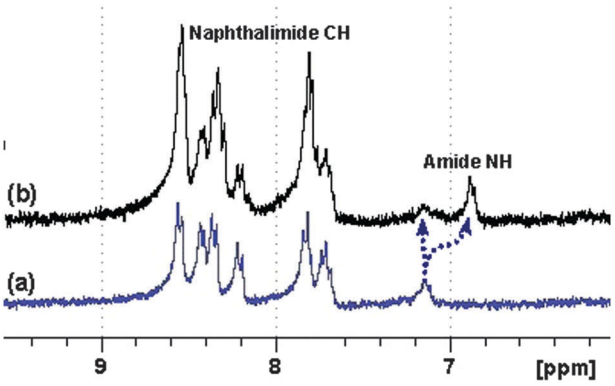

Fig. 7 (a) Partial ^{1}H NMR of **L2**/acetonitrile-d_3 gel at room temperature; and (b) disruption of hydrogen bonds involving the amide NH groups, induced by the addition of 1.0 equiv. of fluoride anions.

gelator molecules, apparently initiated by the coordination of the fluoride anion to the amide NH groups (Fig. 7).

Further support for the effects of TBAF on the gel-to-sol transformation (Scheme 2), and the stimuli-responsive nature of the bis-naphthalimides, **L1** and **L2**, could be obtained from ^{1}H NMR studies. As evident from the ^{1}H NMR spectra, the addition of TBAF (1.0 equiv.) to the **L2**/acetonitrile gel caused the shifting of the amide NH resonance from 7.15 to 6.87 ppm, along with splitting (Fig. 7). The addition of 10 equiv. of TBAF was accompanied by a gradual dissolution and collapse of the organogel network. This effect of TBAF on the hydrogen bonding network of the **L2**–chloroform system could be identified by the disappearance of the absorption at 3304 cm^{-1} in the FTIR spectra. Moreover, the FTIR spectra of **L2** exhibited distinct features due to intra- and intermolecular hydrogen bonding interactions involving the amide NH in solution and in the gel phase absorption. The absorption featured at 3303 cm^{-1} in the FTIR spectra is consistent with intra-molecular hydrogen bonds, and was slightly affected in the gel phase. Accordingly, the ^{1}H NMR spectra of the **L2**–TBAF system in chloroform revealed distinct downfield shifts for the amide NH resonances, which were in accordance with the formation of a hydrogen bonded **L2**–anion complex (Fig. S20, ESI†). Subsequent ^{1}H NMR studies of the interactions of $NaBF_4$ with **L2** in acetonitrile-d_3 and in dimethyl sulfoxide-d^6 revealed minor upfield shifts for the naphthalimide CH resonances at 7.77 and 8.32 ppm. Such features have often been attributed to anion–π interactions between BF_4^- anions and the naphthalimide motifs.[43]

4. Conclusions

In conclusion, we have synthesised and characterised two cystine-based bis-naphthalimides which form fluorescent gels in acetonitrile, DMF and DMSO. Remarkably, both bis-naphthalimides exhibit fluoride-induced quenching and BF_4^- induced restoration of the excimer emissions, which could be visualized under 365 nm UV-illumination. Such 'off/on' switching of excimer emission for the bis-naphthalimides could also be achieved by the successive addition of 3°-amine and hydrofluoric acid. ^{1}H NMR studies

indicated that the incipient gelation process was driven by hydrophobic and aromatic–π interactions between the naphthalimide motifs, supplemented by hydrogen bonding between the amide NH groups. The addition of fluoride caused disruption of the hydrogen bonds involving the amide NH groups, which led to switching of monomer–excimer fluorescence, and concomitant gel-to-sol transition. Thus, we have illustrated a simple strategy for the design of stimuli-responsive functional materials, wherein the switching of monomer–excimer fluorescence emissions of bis-naphthalimides could be triggered by the introduction anions as chemical stimuli.

Acknowledgements

The authors gratefully acknowledge Department of Science & Technology, India (DST-SR/FTP/CS-102/2007) and University Grants Commission (UGC), India for funding and infrastructure facilities, and CIF-IIT Guwahati for assistance with the SEM analysis.

Notes and references

1 J. Zhang, Q. Zou and H. Tian, *Adv. Mater.*, 2013, **25**, 378–399.
2 (*a*) X. Yang, G. Zhang and D. Zhang, *J. Mater. Chem.*, 2012, **22**, 38–50; (*b*) S.-H. Hwang, C. N. Moorefield and G. R. Newkome, *Chem. Soc. Rev.*, 2008, **37**, 2543–2557.
3 (*a*) J. Malinge, C. Allain, A. Brosseau and P. Audebert, *Angew. Chem., Int. Ed.*, 2012, **51**, 8534–8537; (*b*) A. H. Shelton, I. V. Sazanovich, J. A. Weinstein and M. D. Ward, *Chem. Commun.*, 2012, **48**, 2749–2751.
4 (*a*) S. Seo, Y. Kim, Q. Zhou, G. Clavier, P. Audebert and E. Kim, *Adv. Funct. Mater.*, 2012, **22**, 3556–3561; (*b*) D. Kolosov, V. Adamovich, P. Djurovich, M. E. Thompson and C. Adachi, *J. Am. Chem. Soc.*, 2002, **124**, 9945–9954.
5 (*a*) K. Singh, D. Sareen, P. Kaur, H. Miyake and H. Tsukube, *Chem. – Eur. J.*, 2013, **19**, 6914–6936; (*b*) D. Srikun, E. W. Miller, D. W. Domaille and C. J. Chang, *J. Am. Chem. Soc.*, 2008, **130**, 4596–4597.
6 R. M. Duke, E. B. Veale, F. M. Pfeffer, P. E. Kruger and T. Gunnlaugsson, *Chem. Soc. Rev.*, 2010, **39**, 3936–3953.
7 (*a*) L. Zhang, D. Duan, Y. Liu, C. Ge, X. Cui, J. Sun and J. Fang, *J. Am. Chem. Soc.*, 2014, **136**, 226–233; (*b*) B. H. Shankar and D. Ramaiah, *J. Phys. Chem. B*, 2011, **115**, 13292–13299.
8 C. Zhang, Z. Liu, Y. Li, W. He, X. Gao and Z. Guo, *Chem. Commun.*, 2013, **49**, 11430–11432.
9 K. Hanaoka, Y. Muramatsu, Y. Urano, T. Terai and T. Nagano, *Chem. – Eur. J.*, 2010, **16**, 568–572.
10 (*a*) G. T. Spence, M. B. Pitak and P. D. Beer, *Chem. – Eur. J.*, 2012, **18**, 7100–7108; (*b*) V. F. Pais, P. Remon, D. Collado, J. Andreasson, E. Perez-Inestrosa and U. Pischel, *Org. Lett.*, 2011, **13**, 5572–5575.
11 (*a*) H.-H. Lin, Y.-C. Chan, J.-W. Chen and C.-C. Chang, *J. Mater. Chem.*, 2011, **21**, 3170–3177; (*b*) P. A. Panchenko, Y. V. Federova, V. P. Perevalov, J. Gediminas and O. A. Federova, *J. Phys. Chem. A*, 2010, **114**, 4118–4122.
12 (*a*) V. K. Praveen, C. Ranjith and N. Armaroli, *Angew. Chem., Int. Ed.*, 2014, **53**, 365–368; (*b*) L. Maggini and D. Bonifazi, *Chem. Soc. Rev.*, 2012, **41**, 211–241; (*c*) D. W. Domaille, E. L. Que and C. J. Chang, *Nat. Chem. Biol.*, 2008, **4**, 168–175.
13 (*a*) S. S. Babu, V. K. Praveen and A. Ajayaghosh, *Chem. Rev.*, 2014, **114**, 1973–2129; (*b*) K. K. Kartha, R. D. Mukhopadhyay and A. Ajayaghosh, *Chimia*, 2013, **67**, 51–63; (*c*) S. S. Babu, K. K. Kartha and A. Ajayaghosh, *J. Phys. Chem. Lett.*, 2010, **1**, 3413–3424.
14 (*a*) X. Yu, L. Chen, M. Zhang and T. Yi, *Chem. Soc. Rev.*, 2014, **43**, 5346–5371; (*b*) H. Kar, M. R. Molla and S. Ghosh, *Chem. Commun.*, 2013, **49**, 4220–4222; (*c*) D. R. Trivedi and P. Dastidar, *Chem. Mater.*, 2006, **18**, 1470–1478; (*d*) T. Kato, N. Mizoshita and K. Kishimoto, *Angew. Chem., Int. Ed.*, 2006, **45**, 38–68.
15 (*a*) K. V. Rao, K. K. R. Datta, M. Eswaramoorthy and S. J. George, *Adv. Mater.*, 2013, **25**, 1713–1718; (*b*) R. Rajaganesh, A. Gopal, T. M. Das and A. Ajayaghosh, *Org. Lett.*, 2012, **14**, 748–751; (*c*) P. Duan, Y. Li, L. Li, J. Deng and M. Liu, *J. Phys. Chem. B*, 2011, **115**, 3322–3329.
16 (*a*) X. Yu, L. Chen, M. Zhang and T. Yi, *Chem. Soc. Rev.*, 2014, **43**, 5346–5371; (*b*) R. Afrasiabi and H.-B. Kraatz, *Chem. – Eur. J.*, 2013, **19**, 1769–1777; (*c*) G. Cravotto and P. Cintas, *Chem. Soc. Rev.*, 2009, **38**, 2684–2697.
17 (*a*) M. D. Segarra-Maset, V. J. Nebot, J. F. Miravet and B. Escuder, *Chem. Soc. Rev.*, 2013, **42**, 7086–7098; (*b*) T. Kar, S. Dutta and P. K. Das, *Soft Matter*, 2010, **6**, 4777–4787; (*c*) A. Karmakar, R. J. Sarma and J. B. Baruah, *CrystEngComm*, 2007, **9**, 379–389.
18 (*a*) P. Rajamalli, S. Atta, S. Maity and E. Prasad, *Chem. Commun.*, 2013, **49**, 1744–1746; (*b*) J. A. Foster, M.-O. M. Piepenbrock, G. O. Lloyd, N. Clarke, J. A. K. Howard and J. W. Steed, *Nat. Chem.*, 2010, **2**, 1037–1043; (*c*) S.-i. Kawano, N. Fujita and S. Shinkai, *J. Am. Chem. Soc.*, 2004, **126**, 8592–8593.
19 (*a*) W. Edwards and D. K. Smith, *Chem. Commun.*, 2012, **48**, 2767–2769; (*b*) Z. Xu, J. Yoon and D. R. Spring, *Chem. Commun.*, 2010, **46**, 2563–2565.
20 T. C. Barros, P. B. Filho, V. G. Toscano and M. J. Politi, *J. Photochem. Photobiol., A*, 1995, **89**, 141–146.
21 D. W. Cho, M. Fujitsuka, A. Sugimoto and T. Majima, *J. Phys. Chem. A*, 2008, **112**, 7208–7213.
22 G. Loving and B. Imperiali, *J. Am. Chem. Soc.*, 2008, **130**, 13630–13638.
23 (*a*) S. Banerjee, E. B. Veale, C. M. Phelan, S. A. Murphy, G. M. Tocci, L. J. Gillespie, D. O. Frimannsson, J. M. Kelly and T. Gunnlaugsson, *Chem. Soc. Rev.*, 2013, **42**, 1601–1618; (*b*) X. Guo, X. Qian and L. Jia, *J. Am. Chem. Soc.*, 2004, **126**, 2272–2273.
24 Y. Wang, F. Geng, Q. Cheng, H. Xu and M. Xu, *Analyst*, 2011, **136**, 4284–4288.
25 X. Qian, Y. Xiao, Y. Xu, X. Guo, J. Qian and W. Zhu, *Chem. Commun.*, 2010, **46**, 6418–6436.
26 Z. Zhang, D. Wu, X. Guo, X. Qian, Z. Lu, Q. Xu, Y. Yand, L. Duan, Y. He and Z. Feng, *Chem. Res. Toxicol.*, 2005, **18**, 1814–1820.
27 D. W. Cho, M. Fujitsuka, K. H. Choi, M. J. Park, U. C. Yoon and T. Majima, *J. Phys. Chem. B*, 2006, **110**, 4576–4582.

28 J. K. Nath and J. B. Baruah, *Inorg. Chem. Front.*, 2014, **1**, 342–351.
29 (*a*) Q. Song, A. Bamesberger, L. Yang, H. Houtwed and H. Cao, *Analyst*, 2014, **139**, 3588–3592; (*b*) R. J. Sarma, C. Tamuly, N. Barooah and J. B. Baruah, *J. Mol. Struct.*, 2007, **829**, 29–36.
30 S. McMasters and L. Kelly, *J. Phys. Chem. B*, 2006, **110**, 1046–1055.
31 G. Jones II and S. Kumar, *J. Photochem. Photobiol., A*, 2003, **160**, 139–149.
32 R. Ferreira, P. Remon and U. Pischel, *J. Phys. Chem. A*, 2009, **113**, 5805–5811.
33 For **L1** and **L2**, characteristic monomer/excimer emissions were observed in MeCN, THF and DMF.
34 M. Licchelli, A. O. Biroli, A. Poggi, D. Sacchi, C. Sangermani and M. Zema, *Dalton Trans.*, 2003, 4537–4545.
35 Since amines are known to quench naphthalimide fluorescence *via* PET processes: J.-Q. Li and X.-Y. Li, *J. Phys. Chem. A*, 2007, **111**, 13061–13068.
36 M. Kluciar, R. Ferreira, B. de Castro and U. Pischel, *J. Org. Chem.*, 2008, **73**, 6079–6085.
37 X. Tian, Z. Dong, Y. Huang and J. Ma, *Colloids Surf., A*, 2011, **387**, 29–34.
38 M.-L. He, S. Wu, J. He, Z. Abliz and L. Xu, *RSC Adv.*, 2014, **4**, 2605–2608.
39 S.-n. Uno, C. Dohno, H. Bittermann, V. L. Malinovskii, R. Haner and K. Nakatani, *Angew. Chem., Int. Ed.*, 2009, **48**, 7362–7365.
40 Using Benesi–Hildebrand method, the binding constants (K_a) for **L1** and **L2** with fluoride were found to be 8.4×10^4 M^{-1} (**L1**/TBAF) and 9.8×10^4 M^{-1} (**L2**/TBAF); similarly, for **L1**/$NaBF_4$ and **L2**/$NaBF_4$, the K_a values were found to be 5.7×10^4 M^{-1} and 2.6×10^4 M^{-1} respectively; H. A. Benesi and J. H. Hildebrand, *J. Am. Chem. Soc.*, 1949, **71**, 2703–2707.
41 J. Wang, L. Yang, C. Hou and H. Cao, *Org. Biomol. Chem.*, 2012, **10**, 6271–6274.
42 Z. Xu, S. Kim, H. N. Kim, S. J. Han, C. Lee, J. S. Kim, X. Qian and J. Yoon, *Tetrahedron Lett.*, 2007, **48**, 9151–9154.
43 As shown in Fig. S24 (ESI†), interactions of **L2** with $NaBF_4$ in DMSO-d_6 caused perceptible complexation-induced upfield shifts for the naphthalimide CH resonances. However, in acetonitrile-d_3 as solvent, the interaction studies of **L2** with $NaBF_4$ were inconclusive, apparently due to rapid gel formation, and limited solubility of the salt. It may be noted that recent reports suggest that BF_4^- and PF_6^- anions have discernable anion–π interactions with hetero-aromatics, including electron deficient systems: B. L. Schottel, H. T. Chifotides and K. R. Dunbar, *Chem. Soc. Rev.*, 2008, **37**, 68–83.
44 However, chloride, bromide and iodide anions were unable to restore the excimer emission of the fluoride–bis-naphthalimide system under the given conditions.
45 Fig. S11 (ESI†) show the variation in **L2** emissions, in solution and in the gel conditions. Gels produced by **L2** were thermo-reversible. FT-IR studies indicated that the gelator molecules were extensively hydrogen bonded in the gel phase, *via* the amide groups (Fig. S16–S18, ESI†). However, the poor solubility of **L1** in chloroform and acetonitrile prevented similar analysis; solubility of **L1** was $\ll 1$ mg mL^{-1}.
46 X. Yu, Q. Liu, J. Wu, M. Zhang, X. Cao, S. Zhang, Q. Wang, L. Chen and T. Yi, *Chem. – Eur. J.*, 2010, **16**, 9099–9106.
47 (*a*) X. Zhang, S. Lee, Y. Liu, M. Lee, J. Yin, J. L. Sessler and J. Yoon, *Sci. Rep.*, 2014, **4**, 4593; (*b*) J. Wu, T. Yi, Q. Xia, Y. Zou, F. Liu, J. Dong, T. Shu, F. Li and C. Huang, *Chem. – Eur. J.*, 2009, **15**, 6234–6243; (*c*) Y. E. Shapiro, *Prog. Polym. Sci.*, 2011, **36**, 1184–1253.
48 Such features have been noted earlier in aromatic systems following aggregate-formation; (*a*) J. M. Malicka, A. Sandeep, F. Monti, E. Bandini, M. Gazzano, C. Ranjith, V. K. Praveen, A. Ajayaghosh and N. Armaroli, *Chem. – Eur. J.*, 2013, **19**, 12991–13001; (*b*) N. Brosse, D. Barth and B. Jamart-Gregoire, *Tetrahedron Lett.*, 2004, **45**, 9521–9522; (*c*) J. K. Rice, E. D. Niemeyer, R. A. Dunbar and F. V. Bright, *J. Am. Chem. Soc.*, 1995, **117**, 5832; (*d*) J. B. Birk, *Photophysics of Aromatic Molecules*, Wiley-Interscience, New York, 1970.